VOLUME 36 NUMBER 5
MAY 2018

ISSN: 1002-0721
CODEN JREAE 6

# Journal of Rare Earths

ELSEVIER

Project for Enhancing International Impact of China STM Journals

JRE

CONTENTS

## SPECTROSCOPY, LUMINESCENCE AND PHOSPHORS



## ADVANCED RARE EARTH MATERIALS



## CHEMISTRY AND HYDROMETALLURGY



## RARE EARTH APPLICATIONS



## GEOLOGY AND ORE DRESSING



## CORRIGENDUM

**JOURNAL OF RARE EARTHS**

**Vol. 36 No. 5 (May 2018)**

## CONTENTS

### SPECTROSCOPY, LUMINESCENCE AND PHOSPHORS



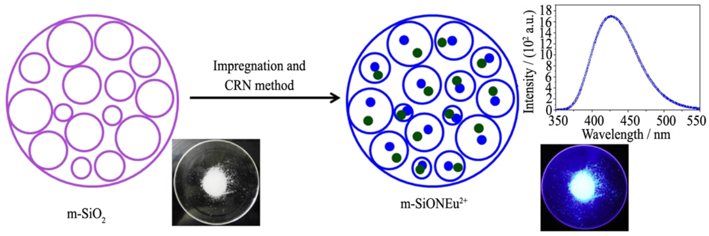


Blue luminescent $Eu^{2+}$-doped mesoporous silicon oxy-nitride materials were synthesized *via* impregnation, nanocasting and, carbothermal reduction and nitridation method. The mesoporous of silicon oxy-nitride act as a host to successfully isolate the luminescent $Eu^{2+}$ ions into the pores and prevent them from aggregation and hence enhanced the luminescent emission efficiency



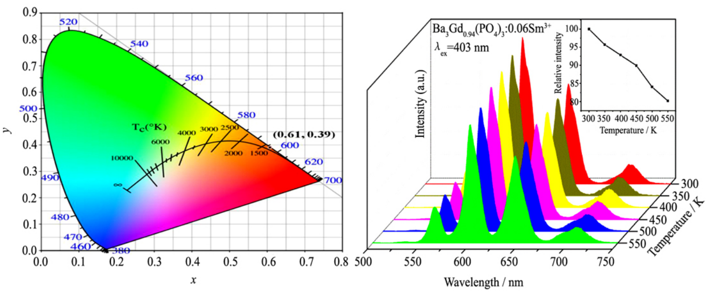


Anovel orange-red emitting phosphor$Ba_3Gd_{0.94}(PO_4)_3$:0.06$Sm^{3+}$ with high thermal stability under near-UV light excitation



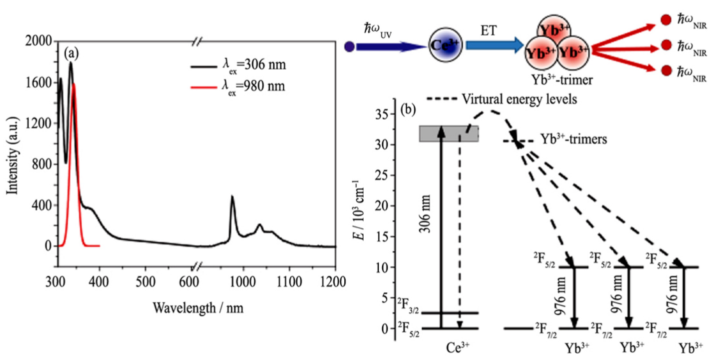


(a) Down conversion emission spectrum (black line) and upconversion emission spectrum (red line) of $CaF_2$:$Yb^{3+}$, $Ce^{3+}$, $Na^+$ excited by 306 nm and 980 nm, respectively; (b) Schematic energy level diagram of $Yb^{3+}$ and $Ce^{3+}$, as well as the proposed QC mechanisms under 306 nm excitation



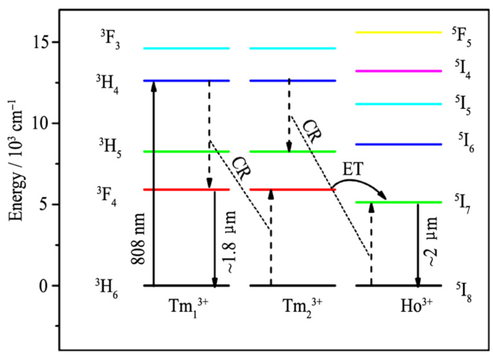


Efficient energy transfer (ET) from $Tm^{3+}$ to $Ho^{3+}$ under the excitation of 808 nm can be achieved in $Y_2O_3$

474 Asymmetry ratio as a parameter of $Eu^{3+}$ local environment in phosphors

*Ilya E. Kolesnikov, Alexey V. Povolotskiy, Daria V. Mamonova, Evgeny Yu. Kolesnikov, Alexey V. Kurochkin, Erkki Läderanta, Mikhail D. Mikhailov*

*J. Rare Earths,* (36) 2018: 474-481

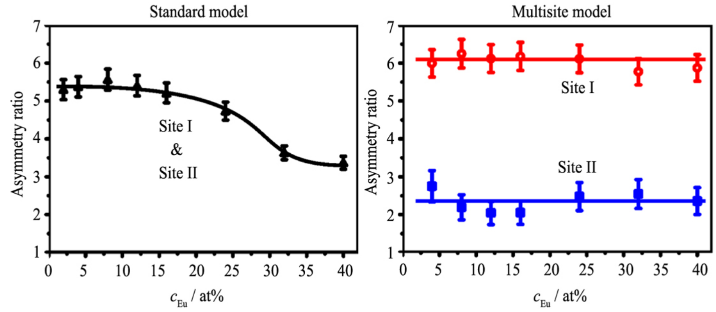


Asymmetry ratio as a function of $Eu^{3+}$ doping concentration for $Y_2O_3:Eu^{3+}$ NPs calculated using standard and multisite models

482 Optical and luminescence characteristics of $Eu^{3+}$-doped $B_2O_3:SiO_2:Y_2O_3:CaO$ glasses for visible red laser and scintillation material applications

*Pabitra Aryal, C.R. Kesavulu, H.J. Kim, S.W. Lee, Sang Jun Kang, J. Kaewkhao, N. Chanthima, B. Damdee*

*J. Rare Earths,* (36) 2018: 482-491

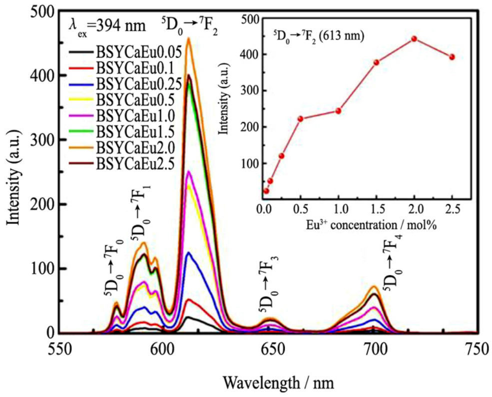


Room temperature emission spectra of $Eu^{3+}$ doped BSYCaEu glasses. Inset shows the emission intensity of dominant $^5D_0 \rightarrow {}^7F_2$ transition as a function of concentration of $Eu^{3+}$ ions

**ADVANCED RARE EARTH MATERIALS**

492 Solid-state reaction synthesis and chemical stability studies in Nd-doped zirconolite-rich ceramics

*Dan Yin, Kuibao Zhang, Le Peng, Zongsheng He, Yuan Liu, Haibin Zhang, Xirui Lu*

*J. Rare Earths,* (36) 2018: 492-498

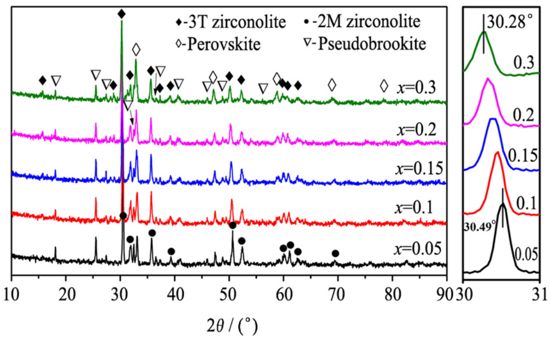


XRD patterns of Nd-doped samples with $x$=0–0.3

Nd-doped zirconolite-rich ceramics were prepared by the solid-sate reactions. Three major phases, namely zirconolite, perovskite and pesudobrookite, were observed in all these samples. Structural transition from monoclinic (2M-$CaZrTi_2O_7$) to trigonal (3T-$CaZrTi_2O_7$) happens when the $Nd_2O_3$ doping content is 7.41 wt%–10.95 wt%. In addition, the trace of $Nd_2O_3$ was not detected in all these samples, suggesting that $Nd_2O_3$ was successfully immobilized into the lattice structure as solid solution. The peaks of zirconolite gradually shift to the lower angle with the increase of $Nd_2O_3$ content. In accordance to Scherrer equation, it is reasonable to deduce that the change of average ionic radius leads to the increment of lattice constant

499 Perovskite type lanthanum manganite: Morpho-structural analysis and electrical investigations

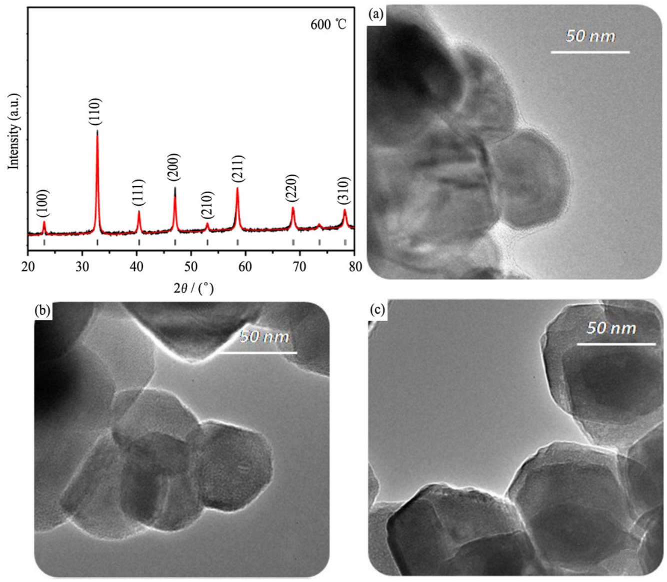


*Paula Sfirloaga, Maria Poienar, Iosif Malaescu, Antoanetta Lungu, Paulina Vlazan*

Rietveld refinement for $LaMnO_3$ heat-treated at 600 °C and TEM image for $LaMnO_3$ heat-treated at different temperatures: 400 °C (a), 600 °C (b), 800 °C (c)

*J. Rare Earths*, (36) 2018: 499-504

## CHEMISTRY AND HYDROMETALLURGY

505 Solubilization behaviors of interfacial lutetium-extractant complex in a solvent extraction system

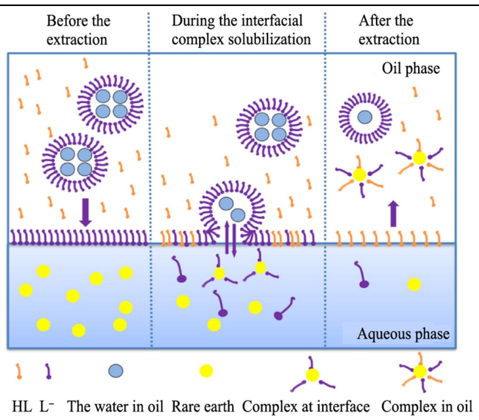


*Wenrou Su, Ji Chen, Yu Jing, Chuanying Liu, Yuefeng Deng, Maohua Yang*

The solubilization of the RE interfacial complex is accompanied with the transfer of solubilized water from microemulsion to aqueous phase

*J. Rare Earths*, (36) 2018: 505-512

513 Rapid recovery of rare earth elements in industrial wastewater by $CuFe_2O_4$ synthesized from Cu sludge

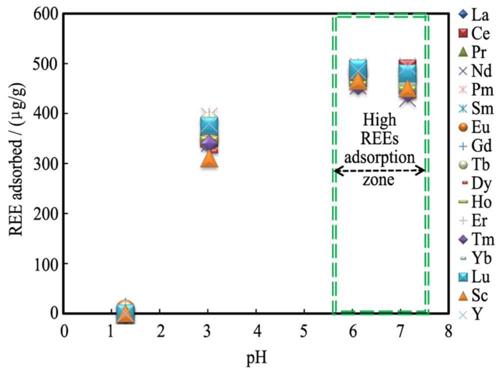


*Yao-Jen Tu, Cliff T. Johnston*

REEs adsorption tendency on magnetic nanoparticles $CuFe_2O_4$ and various pH

*J. Rare Earths*, (36) 2018: 513-520

521 Recovery of rare earths from ion-absorbed rare earths ore with $MgSO_4$-ascorbic acid compound leaching agent

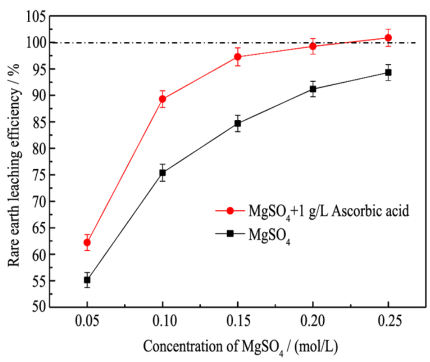


*Fuguo Lai, Li Huang, Guohua Gao, Run Yang, Yanfei Xiao*

The optimum leaching condition in $MgSO_4$-ascorbic acid leaching system leaded to 107.5% of rare earth leaching efficiency and 5.77% Ce partition in the leaching liquor. The leaching efficiency of colloid sediment phase rare earth was up to 85.7%. This method would reduce the consumption of $MgSO_4$ and achieve the simultaneous leaching of colloidal sediment phase and ion-exchangeable phase rare earth. It would have great significance to environmental-friendly extraction of ion-adsorption type rare earths ore and the improvement of resource utilization

*J. Rare Earths*, (36) 2018: 521-527

528 Recovery of rare-earth metal neodymium from aqueous solutions by poly-γ-glutamic acid and its sodium salt as biosorbents: Effects of solution pH on neodymium recovery mechanisms

*Misaki Hisada, Yoshinori Kawase*

*J. Rare Earths,* (36) 2018: 528-536

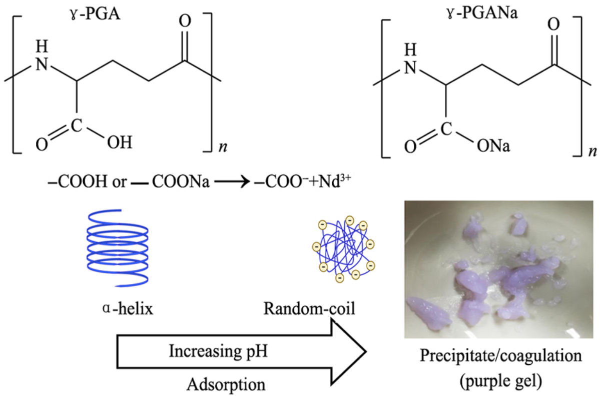


Mechanisms for recovery of rare-earth metal neodymium by poly-γ-sluta mic acid and its sodium salt

537 Synthesis and thermal behavior of $[Li(thf)_3(\mu\text{-}Cl)La\{N(SiMe_3)_2\}_3]$ and its investigation as spin-coating precursor for lanthanum-based layer formation

*Andrea Preu, Elaheh Pousaneh, Julian Noll, Tobias Rüffer, Alexander Jakob, Lutz Mertens, Michael Mehring, Heinrich Lang*

*J. Rare Earths,* (36) 2018: 537-543

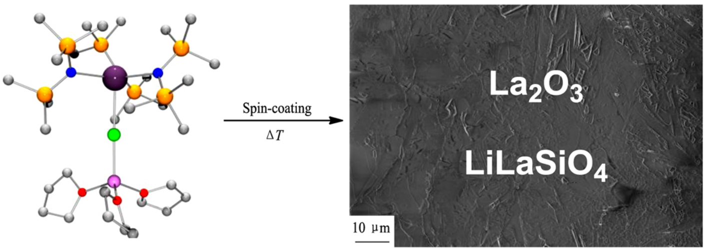


The lanthanum(III) complex $[Li(thf)_3(\mu\text{-}Cl)La\{N(SiMe_3)_2\}_3]$ was synthesized and applied as spin-coating precursor for $La_2O_3$ thin film formation giving the as-deposited layers nearly crack-free

## RARE EARTH APPLICATIONS

544 Study on preparation and properties of $CeO_2$/epoxy resin composite coating on sintered NdFeB magnet

*Pengjie Zhang, Minggang Zhu, Wei Li, Guangqing Xu, Xiulian Huang, Xiaofei Yi, Jingwu Chen, Yucheng Wu*

*J. Rare Earths,* (36) 2018: 544-551

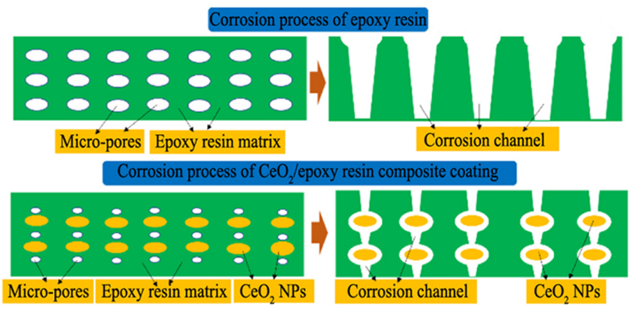


With $CeO_2$ NPs addition, the porosity of the coating decreases, and the density of $CeO_2$/epoxy resin coating is higher than that of blank epoxy resin coatings. And the corrosion channel of the $CeO_2$/epoxy resin composite coating is longer and more tortuous than that of epoxy resin coating due to the blocking effect of $CeO_2$ NPs

## GEOLOGY AND ORE DRESSING

552 Local concentration of middle and heavy rare earth elements in the col on the weathered crust elution-deposited rare earth ores

*Zhenyue Zhang, Ningjie Sun, Zhengyan He, Ru'an Chi*

*J. Rare Earths,* (36) 2018: 552-558

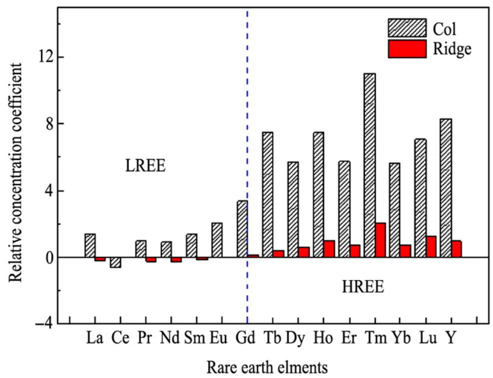


Concentration factor of REEs in different terrain of weathered orebody

# Journal of Rare Earths

## Volume 36, Number 5, May 2018

## Table of Contents